

MASS SCALE EFFECTS IN THE PARTON MODEL

BY D. M. SCOTT*

Rutherford Laboratory, Chilton, Didcot

(Presented at the XVII Cracow School of Theoretical Physics, Zakopane, May 27 — June 9, 1977)

Using parton models which scale asymptotically, we discuss the role of parton and target masses in the approach to scaling, the transverse momentum of partons, and the shape of the structure functions.

1. Introduction

The scaling hypothesis in deep inelastic lepton scattering [1] has been the centre of considerable interest for several years. It is now known from experiments using e , μ , ν and $\bar{\nu}$ as projectiles that scaling is violated, but a complete theory for the violations is lacking¹. A popular explanation is asymptotic freedom [3] (AF), which certainly gives the qualitative, and perhaps quantitative behaviour of the electron and muon scattering data [4]. It is not yet clear whether the same is true for ν , $\bar{\nu}$ scattering, where a new, bottom, quark with right-handed couplings may be needed [5].

The parton model [6], with its pointlike couplings between electromagnetic or weak currents and quark-partons, gives exact scaling asymptotically. However it is relevant to ask how any parton model approaches its asymptotic form, as this may be the source of important scaling violation effects. Here we discuss two approaches to this problem. The first emphasises the importance of charm production in deep inelastic electron and muon scattering. In the second we investigate the effects of the masses of the partons and hadrons involved, first in deep inelastic lepton production, and secondly in high energy hadroproduction of massive lepton pairs. We conclude that these mass scale effects may generate a substantial proportion of the scaling violations observed in lepton production.

The masses of the interacting particles can also play an important role in determining the asymptotic shapes of quantities which scale. In particular the mean square transverse momentum of partons $\langle k_T^2 \rangle$ has been the subject of a number of recent investigations. The dependence of $\langle k_T^2 \rangle$ on the parton's fractional longitudinal momentum x is still not certain. First we discuss the experimental importance of $\langle k_T^2 \rangle$. Then we have a look at it

* Mailing address: Department of Physics, University of Wisconsin, Madison, WI 53706, USA.

¹ A list of possible candidates has been discussed in Ref. [2].

in a simple parton model, and in a simple sum rule for the mean square charge radius of the neutron, finding an interesting conflict. Last of all we show how parton and target masses can affect the shapes of structure functions, using the same simple parton model. In particular, we show how a structure function which behaves like $F_2(x) \sim (1-x)^3$ as $x \rightarrow 1$ can look like $F_2(x) \sim (1-x)^4$ for $x \leq 0.85$, which is the relevant experimental range.

2. The approach to scaling

In Fig. 1 we show the diagram for deep inelastic lepton production, where momenta are defined. We define the usual variables

$$\begin{aligned} p^2 &= M^2, & Q^2 &= -q^2, & \nu &= p \cdot q, \\ \omega &= 2\nu/Q^2, & x &= 1/\omega \end{aligned} \quad (2.1)$$

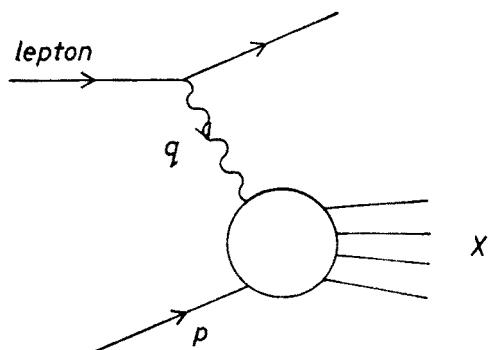


Fig. 1. One photon exchange diagram for deep inelastic lepton scattering

and the usual structure functions

$$\begin{aligned} W_{\mu\nu} &= \frac{1}{4\pi} \int d^4x e^{iq \cdot x} \langle p | [J_\mu(x), J_\nu(0)] | p \rangle \\ &= \left(-g_{\mu\nu} + \frac{q_\mu q_\nu}{q^2} \right) W_1 + \left(p_\mu - \frac{\nu}{q^2} q_\mu \right) \left(p_\nu - \frac{\nu}{q^2} q_\nu \right) \frac{W_2}{M^2}. \end{aligned} \quad (2.2)$$

The scaling hypothesis is

$$W_1 \rightarrow F_1(x), \quad \nu W_2/M^2 \rightarrow F_2(x) \quad (2.3)$$

in the Bjorken limit $\nu \rightarrow \infty$, x fixed.

2.1. The data

Detailed discussions of deep inelastic electron and muon scattering data are given in Ref. [4]. Since then more information from the Chicago-Harvard-Illinois-Oxford (CHIO) collaboration has appeared [7]. The situation is summarised [8] in Fig. 2, where

the structure function $F_2(x)$ is plotted for various values of Q^2 . This behaviour has been neatly parametrised by [8]

$$F_2(x, Q^2) = F_2(x, Q_0^2) (Q^2/Q_0^2)^{f(x)}, \quad (2.4)$$

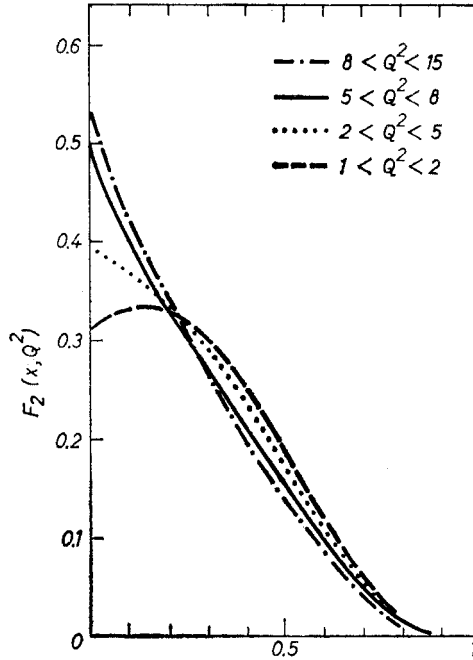


Fig. 2. Behaviour of the structure function $F_2(x)$ for different values of Q^2

where

$$Q_0^2 = 3\text{GeV}^2, \quad f(x) = 0.25 - x, \quad (2.5)$$

which works quite well for $1 < Q^2 < 40 \text{ GeV}^2$.

This shows that as Q^2 increases, F_2 decreases at large x and increases at small x , which is just the AF expectation. Equation (2.4) is not consistent with AF, though.

Finally we note that much detailed quantitative work has been done comparing AF to the data [9]. But here we will look for other sources of scaling violations.

2.2. Is charm production important?

Photoproduction is a good place to look for charm. A charmed baryon has been found there [10], so it must be. Typical estimates give at high energies

$$\frac{\sigma(\gamma N \rightarrow \text{Charm})}{\sigma(\gamma N \rightarrow \text{All})} \simeq 0.3 - 1\%, \quad (2.6)$$

whereas the corresponding fraction in hadroproduction is $(0.3-3) \times 10^{-2} \%$. If this is so, what happens in virtual photoproduction? If we assume scaling, and that the appropriate vector meson sets the mass scale, then

$$\frac{\sigma(\gamma^*(Q^2)N \rightarrow \text{Charm})}{\sigma(\gamma^*(Q^2)N \rightarrow \text{All})} = \frac{1 + (Q^2/m_\rho^2)}{1 + (Q^2/m_\psi^2)} \frac{\sigma(\gamma N \rightarrow \text{Charm})}{\sigma(\gamma N \rightarrow \text{All})} \\ \times \xrightarrow{Q^2 \rightarrow \infty} \frac{m_\psi^2}{m_\rho^2} \frac{\sigma(\gamma N \rightarrow \text{Charm})}{\sigma(\gamma N \rightarrow \text{All})}. \quad (2.7)$$

Note that $m_\psi^2/m_\rho^2 = 16$ is a large number. So when Q^2 increases the signal/noise ratio increases significantly even though the rates for both signal and noise are separately reduced. It is then likely that at high Q^2 the charm cross section in virtual photoproduction will be a substantial part of the total.

In order to be above the charm threshold W_{th} , we require

$$W^2 = (p+q)^2 = M^2 + Q^2(\omega-1) \geq W_{\text{th}}^2. \quad (2.8)$$

So charm is first produced at large W^2 which means large Q^2 and large ω . It gives scaling violations because of the threshold which is fixed in W^2 , and because above threshold scaling is not immediately attained: $\sigma(\gamma^*N \rightarrow \text{Charm}) \sim (Q^2 + m_\psi^2)^{-1}$. So for a fixed beam energy, charm production will affect F_2 at large ω (small x), and will become more important at fixed ω as Q^2 increases. This sort of effect is observed in the data. Let us try to make the discussion a little more quantitative.

In the parton model, we assume that charm is produced from charmed and anti-charmed quarks in the $q\bar{q}$ sea. The strongest assumption about the relative sizes of different components of the sea is SU4 symmetry. This would give a 67% rise across the charm threshold, at small x where the sea is dominant. In analogy to (2.7) we may give the sea quark distributions a Q^2 dependence, with mass scale fixed by the appropriate vector meson:

$$f_i(x, Q^2) = \frac{Q^2}{Q^2 + m_i^2} f_i(x). \quad (2.9)$$

The vector meson is made from quarks \bar{ii} . With this one is able to give a reasonable quantitative explanation of the rise with Q^2 of F_2 at large ω , small x .

So far we have argued by a sequence of guesses. In the next section we try to get somewhat more quantitative results by making a different sequence of guesses in the guise of generalised vector meson dominance (GVMD).

2.3. Just how important?

In reference [11] a detailed GVMD/parton model discussion of $q\bar{q}$ sea distributions is presented. The conclusion is that the Q^2 dependence is given by

$$xf_i(x) = \frac{Q^2}{4m^2} \zeta\left(2, \frac{Q^2 + m^2}{4m^2}\right) f_i(x). \quad (2.10)$$

Here m is the mass of the lightest vector meson made of the bound quarks $i\bar{i}$, Δm^2 is the splitting between that meson and its first radial excitation, and ζ is a generalised Riemann zeta-function

$$\zeta(2, x) = \sum_{n=0}^{\infty} \frac{1}{(n+x)^2} \xrightarrow{x \rightarrow \infty} \frac{1}{x}. \quad (2.11)$$

This shows explicitly that bound state hadronic effects (i.e. vector mesons) control the approach to scaling of the sea distributions in deep inelastic scattering. At asymptotically high energies and momentum transfers, all mass scales are forgotten and the sea becomes SU4 symmetric.

Evidence supporting (2.10) has been presented in Ref. [11]:

- (i) The Michigan State-Cornell-Berkeley-La Jolla [12] 150 GeV μ experiment shows a rise of νW_2 with Q^2 at large ω . This rise is consistent with (2.10).
- (ii) The Chicago-Harvard-Illinois-Oxford [7] 147 GeV μ experiment shows a similar rise and also a fall of νW_2 with ω at large ω ($\omega = 100-1000$). $W_2 \sim Q^2$ for small Q^2 , and high ω at fixed energy implies small Q^2 . The data are consistent with the fall given by equation (2.10).

We now discuss another test for (2.10). This is the rise of νW_2 with Q^2 for $\omega = 9-600$, recently reported by CHIO [13]. They have made a detailed fit [14] to low Q^2 SLAC [15] data using GVMD parametrisations. These parametrisations have a controlling mass scale of $m_\rho^2 - 1 \text{ GeV}^2$, consistent with the data being below charm threshold. The cross sections are separated into diffractive and non-diffractive parts, and from the former we can normalise the sea quark distributions at $Q^2 = \infty$, $\omega = \infty$. This gives

$$\nu W_2/M^2(Q^2, \omega \rightarrow \infty) = 0.26. \quad (2.12)$$

In Ref. [11] we predicted the normalisation $\nu W_2/M^2 = 0.25$ by using (2.10) down to $Q^2 = 0$, and comparing with photoproduction cross section data (this will be explained later). This gives a further test of these ideas. With (2.12),

$$xq(x)|_{x=0} = 0.20. \quad (2.14)$$

We now make the approximation $xq(x) = \text{constant}$ for small x , and simply add in the charm component, with Q^2 dependence given by (2.10). This is relevant at Fermilab energies.

The results are shown in Fig. 3, where the fit to SLAC data is given by the dashed lines. After incorporating charm production we obtain the solid curves. The conclusion is that the rise of $\nu W_2/M^2$ is consistent with the data being above charm threshold, the charm production being controlled by the scale $Q^2 \simeq m_\psi^2$, such that asymptotic SU4 symmetry of the sea obtains as $Q^2 \rightarrow \infty$. The whole of the rise of $\nu W_2/M^2$ at high ω is associated with charm production. This is a crucial difference from AF.

We conclude this section with some remarks [11]:

- (i) The Q^2 dependence given by (2.10) is quite similar to $Q^2/(Q^2 + m_i^2)$.

(ii) Let us make the already mentioned connection with photoproduction, by putting $Q^2 = 0$. The cross section for transverse photon scattering on a nucleon is

$$\sigma_T = \frac{4\pi^2\alpha}{v - \frac{1}{2}Q^2} W_1 = \frac{4\pi^2\alpha}{v - \frac{1}{2}Q^2} \frac{v}{Q^2} \sum e_i^2 x f_i(x, Q^2). \quad (2.15)$$

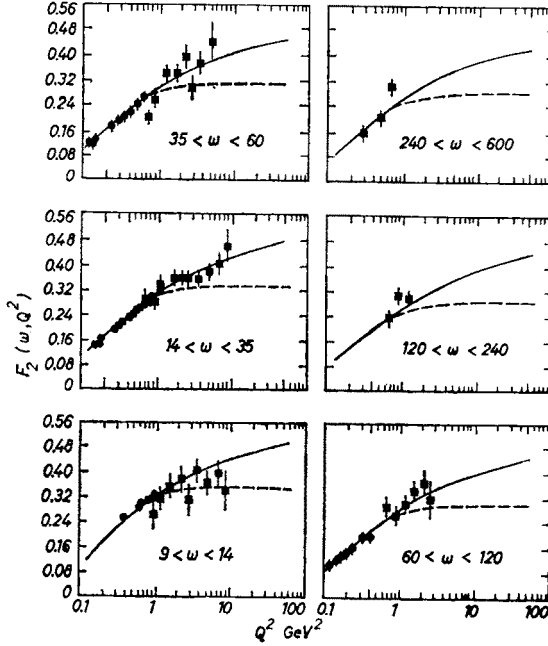


Fig. 3. Data on $eP \rightarrow eX$ (● from SLAC, Ref. [15]), and $\mu P \rightarrow \mu X$ (■ from Fermilab, Ref. [13]). The dashed curve is a fit to SLAC data. The solid curve is the prediction from equation (2.10)

So now we may put $Q^2 = 0$

$$\sigma(\gamma N) = \left\{ 4\pi^2\alpha \sum_i e_i^2 \frac{1}{\Delta m^2} \zeta \left(2, \frac{m^2}{\Delta m^2} \right) \right\} \{xf(x)|_{x=0}\}. \quad (2.16)$$

Putting $\sigma(\gamma N) = 100 \mu\text{b}$ we obtain

$$xf(x)|_{x=0} = 0.19, \quad (2.17)$$

which means that

$$F_2(\omega = \infty) = \begin{cases} 0.25 & \text{below} \\ 0.42 & \text{above} \end{cases} \text{charm threshold}. \quad (2.18)$$

Further if we associate s and \bar{s} with strange production, and c and \bar{c} with charm production, equation (2.16) gives that

$$\begin{aligned} \sigma(\gamma N \rightarrow \text{Strange}) &\simeq 8 \mu\text{b}, \\ \sigma(\gamma N \rightarrow \text{Charm}) &\simeq 2\frac{1}{2} \mu\text{b}. \end{aligned} \quad (2.19)$$

The result for strange production has a little experimental support [16]: for $s = 6\text{--}18 \text{ GeV}^2$, $\sigma(\gamma N \rightarrow \text{Strange}) \simeq 8.5 \text{ } \mu\text{b}$. The result for charm production seems rather large. This is partly so because the contributions from all the ψ 's radial excitations have been added up. The contribution from the ψ (3.1) alone is $\simeq 800 \text{ nb}$.

(iii) Consider electron and neutrino scattering on an average nucleon $N = \frac{1}{2}$ (proton + neutron). For SU3

$$F_2^{\nu N} = \frac{1.8}{5} \left\{ F_2^{eN} - \frac{2x}{9} \frac{s+\bar{s}}{2} - \frac{5x}{9} \sin^2 \theta_c \left(\frac{u+d}{2} - \frac{s+\bar{s}}{2} \right) \right\} \leq \frac{1.8}{5} F_2^{eN}. \quad (2.20)$$

This is the well known result of Llewellyn Smith [17]. Now in SU4,

$$F_2^{\nu N} = \frac{1.8}{5} \left\{ F_2^{eN} + \frac{x}{6} (s+\bar{s}) - \frac{x}{6} (c+\bar{c}) \right\} \begin{cases} = 0, & \text{exact SU4,} \\ \geq \frac{1.8}{5} F_2^{eN}, & \text{if } c = 0. \end{cases} \quad (2.21)$$

So the relation between $F_2^{\nu N}$ and F_2^{eN} depends critically on the kinematic situation, that is how much charm in the sea, and how far above charm threshold. Probably the best that can be said is that as the strange part of the sea is relatively small for most of the x range, $F_2^{\nu N} \simeq \frac{1.8}{5} F_2^{eN}$.

2.4. Let us put in the masses

In this section we study the approach to scaling in the parton model by attempting to take account of parton and hadron masses in calculating the dominant "handbag" diagram, shown in Fig. 4. This exercise has been carried out by many people, both in the

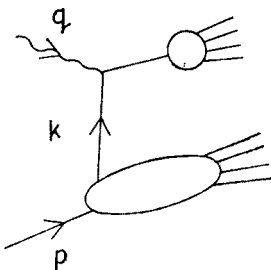


Fig. 4. The dominant parton model "handbag" diagram for deep inelastic lepton scattering

parton model and AF. A discussion and an extensive list of references is given by Barbieri et al. [18]. Here we give a new derivation in a simple parton model [19], and then use the method in the next section to study the approach to scaling in the hadronic production of lepton pairs [19].

We wish to calculate the non-leading terms in Fig. 4. There are two main, and probably related problems: (i) Fig. 4 is only gauge invariant to leading order, and (ii) non-leading terms from diagrams where the parton carrying momentum $(k+q)$ interacts with the system carrying momentum $(p-k)$ may be relevant. We bypass the first problem by calculating

with scalar currents and partons. We cannot say anything about the second problem. Because of this, all we can hope is that the answer gives the qualitative behaviour of the approach to scaling.

After all this, we have to calculate (Fig. 4). We use the covariant parton model [20]. Then

$$vW_2/M^2 = \frac{v}{\pi} \int d^4k \varrho(\sigma) f(k^2, s')$$

$$\sigma = (k+q)^2, \quad s' = (p-k)^2. \tag{2.22}$$

Here ϱ is the spectral function of the parton which has absorbed the current:

$$\int \varrho(\sigma) d\sigma = 1, \tag{2.23}$$

and f is the imaginary part of the forward elastic hadron-parton amplitude. It is convenient to change the integration variables from k to ξ, η and the two-dimensional vector k_T transverse to p and q :

$$k = \left(\xi + \frac{a-1}{2M^2a} \eta \right) p + \frac{\eta}{2va} q + k_T,$$

$$a = \left(1 - \frac{M^2 q^2}{v^2} \right)^{1/2}. \tag{2.24}$$

The nice thing about this is

$$\int d^4k = \frac{1}{2} \int d\xi d\eta d^2k_T,$$

$$k^2 = \xi\eta + \xi^2 M^2 - k_T^2,$$

$$(k-p)^2 = (\xi-1)\eta + (\xi-1)^2 M^2 - k_T^2 = s', \tag{2.25}$$

where we have defined $k_T^2 > 0$. With this change of variables,

$$vW_2/M^2 = \frac{1}{4} \int dk^2 d\xi d\eta dk_T^2 d\sigma ds' \varrho(\sigma) f(k^2, s')$$

$$\times \delta[(\xi-1)\eta + (\xi-1)^2 M^2 - k_T^2 - s'] \delta[s' + \eta + (2\xi-1)M^2 - k^2]$$

$$\times \delta \left[\xi - x + \frac{k^2 - \bar{x}\{k^2 - s' - (2\xi-1)M^2\} - \sigma}{2v} \right], \tag{2.26}$$

where

$$\bar{x} = \frac{2x}{a+1} = x + 0 \left(\frac{1}{v} \right).$$

The only explicit dependence on v is in the last δ -function. We expand this in a Taylor series as

$$\delta \left(A + \frac{B}{v} \right) = \delta(A) + \frac{B}{v} \delta'(A) + \dots \tag{2.27}$$

With this the ξ integration can be performed, yielding

$$\begin{aligned} vW_2/M^2 &= \left(1 - \frac{xM^2}{v}\right) F_2(x) + \frac{\sigma_0 - x^2M^2}{2v} F_2'(x) + 0\left(\frac{1}{v^2}\right) \\ &= \left(1 + \frac{2xM^2}{v}\right)^{1/2} F_2\left(x + \frac{\sigma_0 - x^2M^2}{2v}\right) + 0\left(\frac{1}{v^2}\right), \end{aligned} \quad (2.28)$$

where

$$\begin{aligned} F_2(x) &= \frac{1}{4} \int ds' dk^2 f(k^2, s') \theta(k_T^2) \\ k_T^2 &= -(1-x)k^2 - xs' + x(1-x)M^2, \quad \sigma_0 = \int d\sigma \sigma q(\sigma). \end{aligned} \quad (2.29)$$

This is the same as the results of Ref. [18], where the initial and final partons are put on mass shell. This is not allowed by relativistic kinematics, and differences appear in higher orders. There is a discussion in Ref. [19].

What are the phenomenological consequences of expressions like (2.28)? For large x , and for u, d quarks with (presumably) $m_q^2 \simeq 0.1$,

$$\frac{\sigma_0 - x^2M^2}{2v} < 0. \quad (2.30)$$

The fact that $F_2(x)$ seems to fall quite rapidly as x increases towards 1 means that as Q^2 increases at fixed x , $F_2(x, Q^2)$ falls. The phenomenological analyses of Refs. [18, 20] have suggested that the fall is not fast enough. However, because we are uncertain of the validity of the procedure, we optimistically take this result to be encouraging.

2.5. The Drell-Yan mechanism

The cross section for $pp \rightarrow l^+l^-X$ was first calculated in the parton model by Drell and Yan [22], for the mechanism shown in Fig. 5. The cross section is

$$\frac{d\sigma}{dq^2} = \left(\frac{1}{3}\right) \frac{4\pi\alpha^2}{3q^4} W(\tau = q^2/2v), \quad W = \int dx dy \delta(xy - \tau) \sum e_i^2 F_2^i(x) F_2^{\bar{i}}(y). \quad (2.31)$$

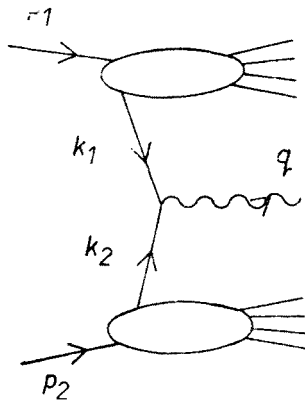


Fig. 5. The dominant parton model Drell-Yan diagram for $pp \rightarrow l^+l^-X$

Here $v = p_1 \cdot p_2$, the factor $(\frac{1}{3})$ is for colour, and the sum is over quarks and anti-quarks.

As in the previous section, we use the covariant parton model [20] to calculate the next to leading order contributions to the dominant diagram, using scalar photon and partons. The problems and uncertainties discussed for lepton production are here too. However, we still calculate [23, 24]

$$W(\tau, v) = \frac{v}{2\pi^2} \int d^4k_1 d^4k_2 f(k_1^2, s'_1) \bar{f}(k_2^2, s'_2) \delta[(k_1 + k_2)^2 - q^2], \quad (2.32)$$

$$s'_i = (p_i - k_i)^2, \quad i = 1, 2.$$

As in (2.22), f is the imaginary part of the forward elastic parton-hadron amplitude. The bar appears on the second function because k_2 is an antiparton.

The calculation of the leading and next to leading terms follows that of the previous section. We find

$$W(\tau, v) = W_0(\tau) + \frac{W_1(\tau)}{2v} + O\left(\frac{1}{v^2}\right), \quad (2.33)$$

where

$$W_0(\tau) = \int dx_1 dx_2 F_2(x_1) \bar{F}_2(x_2) \delta(x_1 x_2 - \tau). \quad (2.34)$$

To find $W_1(\tau)$ we put, for ease,

$$f(k^2, s') = f(k^2) \delta(s' - s'_0) \quad (2.35)$$

and similarly for \bar{f} , and then

$$W_1(\tau) = \frac{1}{\tau} \int dx_1 dx_2 \delta(x_1 x_2 - \tau) \left\{ \frac{x_1^2}{1-x_1} [s_0 - (1-x_1)M_1^2] \frac{\partial}{\partial x_1} \right. \\ \left. + \frac{x_2^2}{1-x_2} [\bar{s}_0 - (1-x_2)M_2^2] \frac{\partial}{\partial x_2} \right\} F_2(x_1) \bar{F}_2(x_2). \quad (2.36)$$

To estimate the magnitude of this correction, we use the parton distributions of Ref. [25]. In Fig. 6 we plot $-W_1(\tau)/W_0(\tau)$ for two choices: $s_0 = \bar{s}_0 = 1$ and $s_0 = s_0 = 4$. Note that the correction is negative, and can be large.

So far in this section our discussion has considered the production of lepton pairs. The Drell-Yan parton-antiparton annihilation mechanism has also been used to describe the hadronic production of J/ψ , which is assumed to couple in a pointlike manner to the parton and antiparton which produce it [25, 26]. At high energies the dominant subprocess is thought to be $c\bar{c} \rightarrow J/\psi$. Taking the charm sea distributions of Ref. [25] we plot $-W_1(\tau)/2vW_0(\tau)$ against s for the two choices of s_0, \bar{s}_0 in Fig. 7. These are the solid lines. To get an estimate of the scale breaking for the Zweig-violating subprocess $q\bar{q} \rightarrow J/\psi$, $q = u, d, s$, we replot the corrections in Fig. 6 for virtual photon production, with $q^2 = 9.58$. This is shown by the dashed lines in Fig. 7. Again the correction is negative, and can be large.

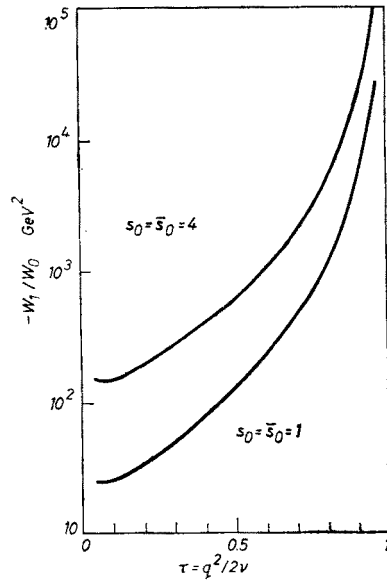


Fig. 6. $-W_1/W_0$ from equations (2.34) and (2.36) for the two choices $s_0 = \bar{s}_0 = 1$, and $s_0 = \bar{s}_0 = 4 \text{ GeV}^2$

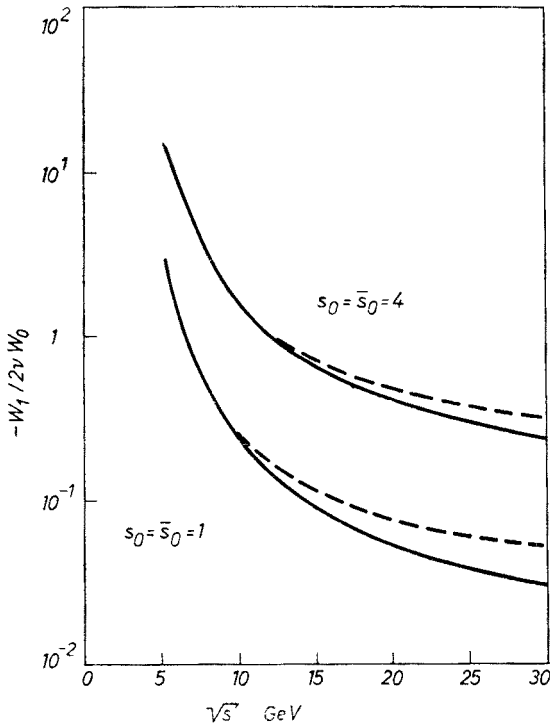


Fig. 7. Corrections $-W_1/2\nu W_0$ for Drell-Yan production of J/ψ . The solid lines are for cc annihilation. The dashed lines are for virtual photon production with $q^2 = 9.58 \text{ GeV}^2$

Note that the sub-asymptotic effects in deep inelastic lepton scattering, and in lepton pair production are controlled by rather different features. For deep inelastic scattering the important parameter is the mass of the parton after it has absorbed the virtual current. For lepton pair production the important feature is how far the partons are off shell before they annihilate. This requires extra information about the dynamics, and is related to the transverse momentum of partons in a hadron, as we will discuss later.

A very simple model has been used, but it is found that the corrections to the Drell-Yan formula, obtained by retaining masses and transverse momenta, can be large. If the estimates we have made are representative, then tests of the Drell-Yan formula at present energies cannot be made very precisely.

3. k_T and F_2

We now consider the shapes of some distributions in the scaling limit. We hope to show that here too the masses of partons and hadrons may play an important role.

3.1. Why is k_T interesting?

Experiments on the hadronic production of high mass lepton pairs [27] have discovered that $\langle p_T \rangle_{l+l-}$ rises with m_{l+l-} , as shown in Fig. 8. If the Drell-Yan mechanism, Fig. 5, is responsible for the production of the lepton pairs, then this can be interpreted

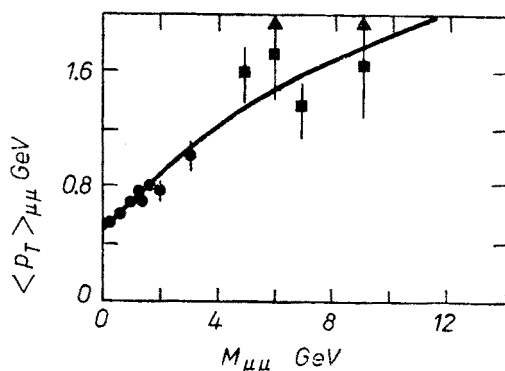


Fig. 8. Data on $pC \rightarrow \mu^+\mu^-X$ at 225 GeV (\bullet), and on $pCu, pBe \rightarrow \mu^+\mu^-X$ at 400 GeV (\blacksquare), Ref. [27]. The curve is from equation (3.4) with $b = 4.5$

to mean that the average transverse momentum of partons in a nucleon increases with increasing x . This can be seen as follows.

The relevant diagram is Fig. 5. Let $k_i \simeq x_i p_i$ for $i = 1, 2$, so that

$$s = (p_1 + p_2)^2 \simeq 2\nu,$$

$$q^2 \simeq (xp_1 + x_2 p_2)^2 \simeq x_1 x_2 \cdot 2\nu, \quad x_F \simeq x_1 - x_2. \quad (3.1)$$

At $x_F \simeq 0$, which is the case experimentally,

$$x_1 \simeq x_2 \simeq q/\sqrt{s}. \quad (3.2)$$

Further,

$$\langle p_T^2 \rangle_{l+l-} = \langle (k_{1T} + k_{2T})^2 \rangle = \langle k_{1T}^2 \rangle + \langle k_{2T}^2 \rangle. \quad (3.3)$$

A rise of $\langle p_T \rangle_{l+l-}$ with q may, via (3.2) and (3.3), be interpreted as a rise of $\langle k_T \rangle$ with x . It can be seen from Fig. 8 that quite high values $\langle k_T \rangle \gtrsim 0.5$ GeV, are required in order to explain the data.

Let us give two warnings about this deduction:

- (i) The effect may not be a rise with x , but simply a rise with q^2 coming from something like AF [28]. Increasing q^2 probes smaller distances, producing greater p_T^2 .
- (ii) The effect may be a manifestation of hadronic mass scales [11]. A typical hadronic parametrisation is

$$\frac{d\sigma}{dp_T^2} \propto e^{-bm_T}, \quad m_T^2 = p_T^2 + q^2. \quad (3.4)$$

This expression gives a $\langle p_T \rangle_{l+l-}$ which increases with q^2 , and the result for $b = 4.5$ is shown in Fig. 8 by the solid line.

In analogy to the scaling hypothesis for deep inelastic lepton scattering, it has been proposed that inclusive hadroproduction cross sections for large p_T secondaries behave as [29]

$$E \frac{d\sigma}{d^3p} \sim \frac{1}{p_T^4} F\left(\frac{p_T}{\sqrt{s}}, 0\right). \quad (3.5)$$

Experimentally the power of p_T^{-1} does not seem to be 4 [30]. For mesons it seems to be $\simeq 8$, and much work has been done on models which yield this power [31].

Recently the CERN-College de France-Heidelberg-Karlsruhe group [32], as well as producing data in support of high p_T jets, proposed a detailed model for hadroproduction at high p_T . This model is based on quark-quark scattering by vector gluon exchange, so that asymptotically (3.5) holds. But the transverse momentum spectrum of the initial quarks is wider than expected. A specific calculation [32] with $\langle k_T \rangle \simeq 3/4$ GeV suggested that in the range of p_T measured $2 < p_T < 5$, the effective power of (p_T^{-1}) is 8. The assumptions and approximations used are now under scrutiny in many places. However it is clear that a careful study of the effects of parton transverse momenta in high p_T physics is required. The first attempts have shown that this may be important phenomenologically.

3.2. What k_T did

Attempts have been made to estimate $k_T(x)$ in the parton model [33–35] Fig. 4. The fact that the parton carrying momentum k is off shell means that its average transverse momentum depends on x , its fractional longitudinal momentum. We have already calculated Fig. 4 in the Bjorken limit, Eq. (2.29). After putting in a factor x for spin [20] and dropping numerical factors we get

$$F_2(x) = x \int ds' dk^2 f(k^2, s') \theta(k_T^2), \quad k_T^2 = -(1-x)k^2 - xs' + x(1-x)M^2. \quad (3.6)$$

We reiterate that this is a scaling result, and that we are not considering subasymptotic corrections.

The next step [34] is to make a simple model for the forward elastic hadron-parton amplitude f :

$$f = \frac{C\delta(s' - s_0)}{(-k^2 + m_0^2)^4}. \quad (3.7)$$

This assumes that f has a strong maximum at some value $s' = s_0$ which is independent of x . This cannot be true for all x , for in order to get the appropriate Regge behaviour for $x \rightarrow 0$, $F_2 \sim \text{const.}$, one needs $s' \sim x^{-1}$. However (3.7) may be reasonable for x not too close to 0.

Plugging (3.7) into (3.6) we find

$$\begin{aligned} F_2(x) &= \frac{Cx}{1-x} \int dk_T^2 \left[\frac{1-x}{k_T^2 + A(x)} \right]^4 \\ &= \frac{1}{3} Cx \left[\frac{1-x}{A(x)} \right]^3, \quad A(x) = xs_0 - x(1-x)M^2 + (1-x)m_0^2. \end{aligned} \quad (3.8)$$

Now it is clear why the power of $(-k^2 + m_0^2)^{-1}$ in (3.7) was chosen to be 4. It gives $F_2 \sim (1-x)^3$ as $x \rightarrow 1$. We will return to this later in section 3.5.

From (3.8) we compute

$$\langle k_T^2(x) \rangle = \frac{1}{2} A(x), \quad (3.9)$$

and so in this simple model $\langle k_T^2(x) \rangle$ depends on the two parameters s_0 and m_0^2 , and

$$\langle k_T^2(x=0) \rangle = \frac{1}{2} m_0^2, \quad \langle k_T^2(x=1) \rangle = \frac{1}{2} s_0. \quad (3.10)$$

By making a suitable choice of these masses [34], for example $m_0^2 = 0.1 \text{ GeV}^2$, $s_0 = 4 \text{ GeV}^2$, we make $\langle k_T^2(x) \rangle$ rise monotonically in $[0, 1]$. The calculation is dubious for small x , as we have mentioned, but there we can invoke the $pp \rightarrow \mu^+\mu^-X$ data, to conclude that the average transverse momentum of partons in a hadron increases with x .

From (3.8) we obtain the distribution in k_T^2 at a given value of x

$$\frac{dN(x, k_T^2)}{dk_T^2} = \frac{3[A(x)]^3}{[k_T^2 + A(x)]^4}. \quad (3.11)$$

An exponential form for this distribution is often assumed, but here the power law dependence on k_T^2 follows from the power law behaviour $F_2 \sim (1-x)^3$ and $x \sim 1$. Of course the precise form depends on the details of the model.

3.3. What k_T did next

The mean square charge radius of a nucleon $\langle r^2 \rangle$ is defined in terms of the derivative of the electric form factor:

$$\left. \frac{dG_E}{dQ^2} \right|_{Q^2=0} = -\frac{\langle r^2 \rangle}{6}. \quad (3.12)$$

It is a common belief, which we do not question here, that this definition is equivalent to the non-relativistic definition

$$\langle r^2 \rangle = \int d^3r \varrho(r) r^2, \quad (3.13)$$

where $\varrho(r)$ is the charge density at the point r . Experimentally [36],

$$\langle r^2 \rangle_p \simeq 0.70 \text{ fm}^2 = 18.0 \text{ GeV}^{-2}, \quad \langle r^2 \rangle_N \simeq -0.12 \text{ fm}^2 = -3.1 \text{ GeV}^{-2}. \quad (3.14)$$

There has been some difficulty in quark models in obtaining $\langle r^2 \rangle_N < 0$ from (3.13), though by now several explanations have been proposed [37]. Here we will use a rule first written down by Pavkovic [38], and used in the present context by Sehgal [39].

Partons in a hadron are described by probability distributions $f_i(x)$ from which we obtain the structure functions

$$F_1 = \frac{1}{2x} F_2 = \frac{1}{2} \sum e_i^2 f_i(x).$$

The charge of the target t is given by

$$Q_t = \sum_i e_i \int_0^1 f_i^t(x) dx. \quad (3.15)$$

So the partons' x dependences are familiar. But partons also have a transverse momentum, or transverse spatial, dependence. Let the position in the transverse plane be given by coordinate \mathbf{r} , and let the distribution of partons in x and \mathbf{r} be given by $h_i(x, \mathbf{r})$ so that

$$h_i(x, \mathbf{r}) = f_i(x) N_i(x, \mathbf{r}). \quad (3.16)$$

Then

$$\int h_i(x, \mathbf{r}) d^2\mathbf{r} = f_i(x) \quad (3.17)$$

implies

$$\int N_i(x, \mathbf{r}) d^2\mathbf{r} = 1. \quad (3.18)$$

Just as the target's charge is given by (3.15), so the mean square charge radius is²

$$\begin{aligned} \langle r^2 \rangle &= \frac{3}{2} \int_0^1 dx \int_0^\infty d^2\mathbf{r} r^2 \sum_i e_i h_i(x, \mathbf{r}), \\ &= \frac{3}{2} \sum_i e_i \int_0^1 dx f_i(x) \langle r_{iT}^2(x) \rangle. \end{aligned} \quad (3.19)$$

Here $\langle r_{iT}^2(x) \rangle$ is the mean square transverse radius of parton i at position x .

This is the basic equation. To complete the argument [40] we will make the strongest assumptions, which however may be relaxed a little.

² The factor 3/2 comes from rotational invariance.

First, the $q\bar{q}$ sea contributions in (3.19) are assumed to cancel in pairs. Secondly, by the uncertainty principle,

$$\langle r_{iT}^2(x) \rangle \geq \frac{1}{2\langle k_{iT}^2(x) \rangle}, \tag{3.20}$$

and we further assume that these quantities are independent of parton type i .

Consider now a neutron target N , and let $u_v(x)$ and $d_v(x)$ be the valence u and d quark distributions respectively in a *proton*. Then we have two sum rules from (3.15) and (3.19):

$$0 = \int_0^1 dx \left[\frac{2}{3} d_v(x) - \frac{1}{3} u_v(x) \right],$$

$$\langle r^2 \rangle_N \geq \int_0^1 dx \left[\frac{2}{3} d_v(x) - \frac{1}{3} u_v(x) \right] \frac{1}{2\langle k_T^2(x) \rangle}. \tag{3.21}$$

Some people [25] would like the quantity in brackets to be identically zero. This, however would give $\langle r^2 \rangle_N = 0$, and so we choose the other belief which is $d_v/u_v \rightarrow 0$ as $x \rightarrow 1$

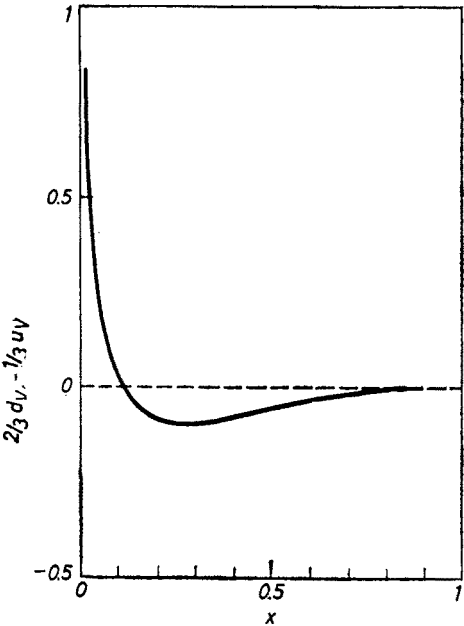


Fig. 9. An estimate of $\frac{2}{3}d_v(x) - \frac{1}{3}u_v(x)$ for the case $d_v/u_v \rightarrow 0$ as $x \rightarrow 0$

With this, $[\frac{2}{3}d_v - \frac{1}{3}u_v]$ is shown schematically in Fig. 9. Note that the areas above and below the x -axis are the same.

Now take the parton model expectation for $\langle k_T^2(x) \rangle$, i.e. $\langle k_T^2(x) \rangle$ rises with x . Then (3.21) gives

$$\langle r^2 \rangle_N \geq 0. \tag{3.22}$$

This is the contradiction.

As we have discussed, there is some evidence from $pp \rightarrow \mu^+ \mu^- X$ that $\langle k_T^2(x) \rangle$ increases with x for small x . In order to get $\langle r^2 \rangle_N \lesssim 0$, we require $\langle k_T^2(x) \rangle$ to decrease for large x , so that the negative part of the integrand, see Fig. 9, may be enhanced in (3.21). It is difficult to be more quantitative. All we can say is that we expect $\langle k_T^2(x) \rangle$ to decrease for $x \gtrsim 0.5$, say.

3.4. Another look at $\langle r^2 \rangle$

The previous section was concerned with the neutron, where small effects and cancellations were in question. Let us turn to situations where this is not so — the proton and π^+ . The basic equation we will use is

$$\langle r^2 \rangle \gtrsim \frac{3}{4} \int_0^1 dx \sum_i e_i f_i(x) \frac{1}{\langle k_T^2(x) \rangle}. \quad (3.23)$$

Even though we expect $\langle k_T^2(x) \rangle$ to depend on x , we may define an average $\langle k_T^2(x) \rangle$ by

$$\begin{aligned} \langle k_T^2 \rangle &\gtrsim \left[\frac{3}{4} \int_0^1 dx \sum_i e_i f_i(x) \right] / \langle r^2 \rangle, \\ &= 0.75 Q_1 / \langle r^2 \rangle. \end{aligned} \quad (3.24)$$

So from (3.14)

$$\langle k_T^2 \rangle_p \gtrsim 0.04 \text{ GeV}^2, \quad (3.25)$$

which is reasonable.

The pion $\langle r^2 \rangle$ is still somewhat uncertain experimentally [41]. Most determinations give $\langle r^2 \rangle_{\pi^+} \simeq 0.5 \text{ fm}^2$, whereas there is a recent Fermilab result [42] $0.33 \pm 0.06 \text{ fm}^2$. Taking the former we find

$$\langle k_T^2 \rangle_\pi \gtrsim 0.06 \text{ GeV}^2, \quad (3.26)$$

which again is quite reasonable.

3.5. The Drell-Yan-West relation

Drell and Yan, and West have proposed a relation [43] (the DYW relation) between the deep inelastic structure functions and the electromagnetic form factors of the nucleon. If $G_M(Q^2) \sim (Q^2)^{-p}$ as $Q^2 \rightarrow \infty$, and $F_2(x) \sim (1-x)^n$ as $x \rightarrow 1$, then

$$n = 2p - 1. \quad (3.27)$$

The common belief is that $p = 2$, and that $n = 3$, in agreement with (3.27). However data [44] from SLAC have suggested the possibility that in fact $n = 4$.

The DYW relation is supposed to hold for $x \rightarrow 1$, but experimentally $x \leq 0.85$. Here we show [19] by a simple example that this may already be too far away from $x = 1$.

We use the simple parton model described earlier in section 3.2, where $F_2(x)$ is given by equation (3.8). Recall that $A(x) = 2\langle k_T^2(x) \rangle$ increases monotonically as x goes from

0 to 1. So $F_2(x)$ falls off *faster* than $(1-x)^3$ as x approaches 1. With the special choices $m_0^2 = 1.24$ and $s_0 = 2.70$ we plot $F_2(x)/x(1-x)^4$ in Fig. 10, finding that this function looks reasonably flat over the experimental range (in fact m_0^2 and s_0 have been chosen to make it flattest). This result is not too sensitive to choice of parameters. For quite a wide range of

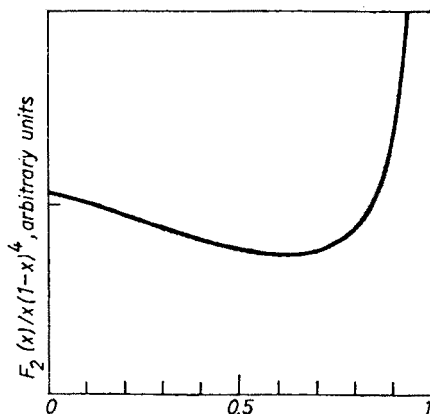


Fig. 10. $F_2(x)/[x(1-x)^4]$. $F_2(x)$ is given by equation (3.8) with the "flattest" choices $m_0^2 = 1.24$, $s_0 = 2.70$. The qualitative shape is fairly insensitive to parameters

m_0^2 and s_0 the power 4 gives a better approximation than the power 3 to F_2 . This is when $A(x)$ is an increasing function of x for x near 1.

To conclude, if it is true at all the DYW relation is expected to hold only for x near to 1. Just how near to 1 is not specified. What we have shown here in a very simple model is that in the presently accessible experimental range $x \leq 0.85$, x is *not* close enough to 1. The effective power of $(1-x)$ is changed from that at threshold $x = 1$.

I wish to thank the organisers for giving me the opportunity to attend the Cracow School. I am most grateful to F. E. Close, F. Halzen, P. V. Landshoff, S. Matsuda and D. Sivers. I thank R. J. N. Phillips for helpful comments on the manuscript.

REFERENCES

- [1] J. D. Bjorken, *Phys. Rev.* **179**, 1547 (1969).
- [2] C. H. Llewellyn Smith, Proceedings of the International Symposium on Lepton and Photon Interactions at High Energies, Stanford 1975.
- [3] H. D. Politzer, *Phys. Rep.* **14C**, 130 (1974).
- [4] See L. Mo, R. Taylor, Proceedings of the International Symposium on Lepton and Photon Interactions at High Energies, Stanford, 1975.
- [5] See A. Buras, CERN preprint TH.2285.
- [6] J. D. Bjorken, E. A. Paschos, *Phys. Rev.* **185**, 1975 (1969); R. P. Feynman, *Photon-Hadron Interactions*, W. A. Benjamin, New York 1972.
- [7] H. L. Anderson et al., *Phys. Rev. Lett.* **37**, 4 (1976); papers submitted to XVIII International Conference on High Energy Physics, Tbilisi 1976.
- [8] D. H. Perkins, P. Schreiner, W. G. Scott, *Phys. Lett.* **67B**, 347 (1977).
- [9] For references see Ref. [5].

- [10] B. Knapp et al., *Phys. Rev. Lett.* **37**, 882 (1976).
- [11] F. E. Close, D. M. Scott, D. Sivers, *Phys. Lett.* **62B**, 213 (1976); *Nucl. Phys.* **B117**, 134 (1976); F. E. Close, D. M. Scott, Rutherford preprint RL-77-058/A.
- [12] Y. Watanabe et al., *Phys. Rev. Lett.* **35**, 898 (1975); C. Chang et al., *Phys. Rev. Lett.* **35**, 901 (1975).
- [13] V. K. Bharadwaj, Ph. D. Thesis, Oxford 1977.
- [14] H. L. Anderson et al., *Generalised Vector Dominance and the Low q^2 μp and μd Inelastic Scattering at 150 GeV*, submitted to XVIII International Conference on High Energy Physics, Tbilisi 1976.
- [15] S. Stein et al., *Phys. Rev.* **D12**, 1884 (1975); SLAC-PUB-1528, 1975; F. M. Riordan et al., SLAC-PUB-1634, 1975.
- [16] K. C. Moffeit et al., *Phys. Rev.* **D5**, 1603 (1972).
- [17] C. H. Llewellyn Smith, *Nucl. Phys.* **B17**, 277 (1970).
- [18] R. Barbieri et al., *Nucl. Phys.* **B117**, 50 (1976).
- [19] P. V. Landshoff, D. M. Scott, preprint DAMTP 77/14.
- [20] P. V. Landshoff, J. C. Polkinghorne, *Phys. Rep.* **5C**, 1 (1972).
- [21] R. K. Ellis, R. Petronzio, G. Parisi, *Phys. Lett.* **64B**, 97 (1976).
- [22] S. D. Drell, T. M. Yan, *Ann. Phys.* **66**, 578 (1971).
- [23] For 2π 's see P. V. Landshoff, H. Osborn, to appear in *Electromagnetic Interactions of Hadrons*, ed. A. Donnachie and G. Shaw, Plenum Publishing Co., CERN-TH-2157.
- [24] P. V. Landshoff, J. C. Polkinghorne, *Nucl. Phys.* **B33**, 221 (1971); erratum *Nucl. Phys.* **B36**, 642 (1971).
- [25] A. Donnachie, P. V. Landshoff, *Nucl. Phys.* **B112**, 233 (1976).
- [26] M. B. Green, M. Jacob, P. V. Landshoff, *Nuovo Cimento* **29A**, 123 (1975); J. F. Gunion, *Phys. Rev.* **D12**, 1345 (1975); D. Sivers, *Nucl. Phys.* **B106**, 95 (1976), to name but a few.
- [27] K. J. Anderson et al., *Phys. Rev. Lett.* **37**, 799 (1976); D. C. Hom et al., *Phys. Rev. Lett.* **37**, 1374 (1976).
- [28] J. B. Kogut, *Phys. Lett.* **65B**, 377 (1976); I. Hinchliffe, C. H. Llewellyn Smith, *Phys. Lett.* **66B**, 281 (1977).
- [29] S. M. Berman, J. D. Bjorken, J. B. Kogut, *Phys. Rev.* **D4**, 3388 (1971).
- [30] See P. Darriulat, XVIII International Conference on High Energy Physics, Tbilisi 1976.
- [31] D. Sivers, S. J. Brodsky, R. Blankenbecler, *Phys. Rep.* **23C**, 1 (1976), contains a review and references.
- [32] CCHK Collaboration: M. Della Negra et al., CERN/EP/PHYS 77-10.
- [33] Minh Duong-van, SLAC-PUB-1819, 1976.
- [34] P. V. Landshoff, *Phys. Lett.* **66B**, 452 (1977).
- [35] J. F. Gunion, Davis preprint UCD-76-8, 1976.
- [36] See G. Höhler et al., *Nucl. Phys.* **B114**, 505 (1976).
- [37] See R. D. Carlitz, S. D. Ellis, R. Savit, RLO-1388-725.
- [38] M. I. Pavkovic, *Phys. Rev.* **D9**, 1054 (1974).
- [39] L. M. Sehgal, *Phys. Lett.* **53B**, 106 (1974).
- [40] F. E. Close, F. Halzen, D. M. Scott, Rutherford preprint RL-77-032/A.
- [41] See C. L. Hammer et al., *Phys. Rev.* **D15**, 696 (1977).
- [42] J. Lach, Fermilab report.
- [43] S. D. Drell, T. M. Yan, *Phys. Rev. Lett.* **24**, 181 (1970); G. B. West, *Phys. Rev. Lett.* **24**, 1206 (1970).
- [44] W. B. Atwood, SLAC-185 (1975).